KIF5B transports BNIP-2 to regulate p38 mitogen-activated protein kinase activation and myoblast differentiation

Peng Yi[a,b,*], Li Li Chew[c,d,*], Ziwang Zhang[a,b,*], Hao Ren[b], Feiya Wang[a,b], Xiaoxia Cong[a,b], Liling Zheng[a], Yan Luo[a], Hongwei Ouyang[b], Boon Chuan Low[c,d], and Yi Ting Zhou[a,b]

[a]Center for Stem Cell and Tissue Engineering, Department of Biochemistry and Molecular Biology, and [b]Zhejiang Provincial Key Lab for Tissue Engineering and Regenerative Medicine, Zhejiang University School of Medicine, Hangzhou 310058, China; [c]Department of Biological Sciences and [d]Mechanobiology Institute, National University of Singapore, 117411 Singapore

ABSTRACT **The Cdo-p38MAPK (p38 mitogen-activated protein kinase) signaling pathway plays important roles in regulating skeletal myogenesis. During myogenic differentiation, the cell surface receptor Cdo bridges scaffold proteins BNIP-2 and JLP and activates p38MAPK, but the spatial-temporal regulation of this process is largely unknown. We here report that KIF5B, the heavy chain of kinesin-1 motor, is a novel interacting partner of BNIP-2. Coimmunoprecipitation and far-Western study revealed that BNIP-2 directly interacted with the motor and tail domains of KIF5B via its BCH domain. By using a range of organelle markers and live microscopy, we determined the endosomal localization of BNIP-2 and revealed the microtubule-dependent anterograde transport of BNIP-2 in C2C12 cells. The anterograde transport of BNIP-2 was disrupted by a dominant-negative mutant of KIF5B. In addition, knockdown of KIF5B causes aberrant aggregation of BNIP-2, confirming that KIF5B is critical for the anterograde transport of BNIP-2 in cells. Gain- and loss-of-function experiments further showed that KIF5B modulates p38MAPK activity and in turn promotes myogenic differentiation. Of importance, the KIF5B-dependent anterograde transport of BNIP-2 is critical for its promyogenic effects. Our data reveal a novel role of KIF5B in the spatial regulation of Cdo–BNIP-2–p38MAPK signaling and disclose a previously unappreciated linkage between the intracellular transporting system and myogenesis regulation.**

Monitoring Editor
Xueliang Zhu
Chinese Academy of Sciences

Received: Mar 12, 2014
Revised: Oct 9, 2014
Accepted: Oct 29, 2014

INTRODUCTION

During the process of cell differentiation, precursor cells respond to external cues by membrane-spanning receptors and trigger a number of downstream signaling pathways. Various mitogen-activated protein kinases (MAPKs) are activated by cascades of protein kinases. Activating these signaling modules at the correct time and subcellular location is critical for cell fate decision. For example, transient epidermal growth factor–dependent MAPK signaling causes PC12 cell proliferation, whereas prolonged nerve growth factor–triggered MAPK activation induces neuronal differentiation (Marshall, 1995). It is believed that scaffold proteins play key roles in precisely regulating signaling modules to achieve such specificity (Dhanasekaran *et al.*, 2007). Indeed, distinct scaffold proteins interact with various MAPK cascade components and bring them to close proximity for efficient signaling propagation (Good *et al.*, 2011; Pan *et al.*, 2012). The characterization of cellular factors involved in spatial-temporal modulation of scaffold proteins thus represents a crucial step toward a better understanding of the regulation of cellular differentiation.

Differentiation of skeletal muscle progenitors into multinucleated myotubes is a multistep process that undergoes dramatic

This article was published online ahead of print in MBoC in Press (http://www.molbiolcell.org/cgi/doi/10.1091/mbc.E14-03-0797) on November 5, 2014.

*These authors contributed equally to this work.

Address correspondence to: Yi Ting Zhou (zhouyt@zju.edu.cn), Boon Chuan Low (dbslowbc@nus.edu.sg).

Abbreviations used: BNIP-2, BCL2/adenovirus E1B 19 kDa protein-interacting protein 2; Cdo, CAM related/down-regulated by oncogenes; DM, differentiation medium; GAP, GTPase-activating protein; GM, growth medium; JLP, c-Jun NH2-terminal kinase-associated leucine zipper proteinl; MHC, myosin heavy chain.

morphological changes and genetic reprogramming (Cole *et al.*, 2004; Tapscott, 2005; Guasconi and Puri, 2009; Bentzinger *et al.*, 2012). This multistage process is under tight control by signal transduction pathways that regulate the p38MAPK activity (Jones *et al.*, 2005). In differentiating myoblasts, p38MAPK is activated to regulate MEF2 transcription factors (Han *et al.*, 1997; Puri *et al.*, 2000; Wu *et al.*, 2000; de Angelis *et al.*, 2005). As one of the key regulatory pathways of p38MAPK activity, Cdo signaling is initiated by cell–cell contact that triggers the ligation of the N-cadherin and Cdo receptor, an orphan receptor of the immunoglobulin (Ig)/fibronectin repeat family (Kang *et al.*, 1998, 2002, 2003). Two scaffold proteins, JLP and BNIP-2, are subsequently recruited by the intracellular region of Cdo (Takaesu *et al.*, 2006; Kang *et al.*, 2008). JLP activates p38MAPK by bridging it with MKK3/6 and in turn promotes myogenesis through phosphorylation of substrates that stimulate muscle-specific, MyoD-dependent gene expression. The other scaffold protein, BNIP-2, also binds Cdo receptor and is involved in regulating p38MAPK activity. The BNIP-2 protein family is characterized by a novel protein–protein interaction domain, the BNIP-2 and Cdc42GAP homology (BCH) domain, in the C-terminus. In addition to the ability to form homophilic and heterophilic complexes (Low *et al.*, 1999, 2000), studies by us and others showed that the BCH domain can target the Rho GTPases and regulate cell dynamics (Pan and Low, 2012). For instance, BNIP-2 binds Cdc42 and causes cell elongation and protrusion (Zhou *et al.*, 2005), whereas BNIP-Sα induces cell rounding and apoptosis by engaging RhoA and displacing its inactivator, p50RhoGAP (Zhou *et al.*, 2002, 2006). As an extension to this, recent studies showed that the endosomal localization of p50RhoGAP is BCH domain dependent (Sirokmany *et al.*, 2006; Zhou *et al.*, 2010), whereas the BCH domain of caytaxin (BNIP-H) mediates its mitochondria localization (Aoyama *et al.*, 2009). These observations suggest that some BNIP-2 family members function as dynamic scaffolds that target signaling proteins to specific cellular compartments to regulate their activities.

Intracellular trafficking is critical for appropriate cellular functions. By hydrolyzing ATP for energy, a group of molecular motors known as the kinesin superfamily proteins (KIFs) transport cargoes, including cellular organelles, protein complexes, and mRNAs, toward the plus end of microtubules (Hirokawa and Noda, 2008; Hirokawa *et al.*, 2009; Verhey and Hammond, 2009). The first KIF to be reported was KIF5, or kinesin heavy chain (KHC), which has three homologous members designated KIF5A, KIF5B, and KIF5C (Vale *et al.*, 1985; Kanai *et al.*, 2000). Conventionally, kinesin-1 refers to a heterotetramer that comprises two kinesin heavy chains and two kinesin light chains (KLCs; Hirokawa *et al.*, 1989; Hirokawa and Noda, 2008). Recent studies revealed the interaction between kinesin-1 and an increasing list of signaling proteins implicated in various biological functions. For instance, the association of RanBP2 with KIF5B and KIF5C determines mitochondria localization (Cho *et al.*, 2007), whereas transporting of Kidins220/ARMS by kinesin-1 is involved in neuronal differentiation (Bracale *et al.*, 2007). In *Drosophila*, KIF5B is involved in nuclear positioning required for skeletal muscle function (Metzger *et al.*, 2012). Further, the brain-specific homologue of BNIP-2, BNIP-H (caytaxin), transports kidney-type glutaminase (Buschdorf *et al.*, 2006) and mitochondria toward neurite termini by forming a complex with kinesin-1 through an interaction with KLC (Aoyama *et al.*, 2009). Based on these observations, we speculate that kinesin-mediated processes could be linked to the regulation of the Cdo–BNIP-2–MAPK pathway during myogenesis.

Here we determine the endosomal localization of BNIP-2 and show that KIF5B is a novel binding partner of BNIP-2. BNIP-2 binds KIF5B via its BCH domain, whereas both motor and tail domains of KIF5B are required for its interaction with BNIP-2. The KIF5B–BNIP-2 interaction is critical for the anterograde transport of BNIP-2. Of importance, the KIF-dependent anterograde transport of BNIP-2 is critical for its promyogenic effects. We further confirmed that KIF5B is required for p38MAPK activation and myoblast differentiation. Taken together, we demonstrated that the KIF5B–BNIP-2 interaction is critical for intracellular transport of BNIP-2 and activation of p38MAPK, thus highlighting a unique link between the transporting motor and the spatial regulation of BNIP-2-mediated Cdo signaling for myogenic differentiation.

RESULTS

KIF5B interacts with BNIP-2

To further explore the function of BNIP-2 and its underlying mechanism of myogenesis, we set out to identify its binding partners by subjecting purified recombinant glutathione *S*-transferase (GST)–BNIP-2 to 293T cells. One unique band of 125 kDa was consistently observed (Figure 1A, asterisks). Tryptic digests and analyses by matrix-assisted laser desorption/ionization time-of-flight (MALDI-TOF) mass spectrometry revealed various peptides that formed different parts of KIF5B (with 22% coverage of total sequence; Figure 1B). To validate their interaction, we coexpressed hemagglutinin (HA)-tagged BNIP-2 and FLAG-tagged KIF5B and showed them to coimmunoprecipitate in 293T cells (Supplemental Figure S1A). Further, FLAG-tagged BNIP-2 could interact with the endogenous KIF5B when the cells were proliferating in growth medium (GM) or over a 2-d time course after their transfer to the differentiation medium (DM; Figure 1C). When determined by quantitative PCR (qPCR) and Western blot, the expression of endogenous KIF5B in C2C12 myoblasts increased during differentiation, similar to the profile of Cdo and JLP (Figure 1, D and E).

To confirm that KIF5B is a bona fide interacting partner of BNIP-2 in vivo under physiological conditions, we first immunoprecipitated endogenous BNIP-2 in dissected mouse hindlimb muscle lysate; both BNIP-2 and KIF5B were present in the precipitate (Figure 1F). Further, cell lysates from the proliferating and differentiating myoblasts were immunoprecipitated with BNIP-2 antibodies and probed for KIF5B. Western blot analysis showed the presence of both endogenous BNIP-2 and KIF5B under both cellular conditions (Figure 1G). As a control, scaffold protein JLP of Cdo-p38MAPK signaling was also present in the precipitate. Thus KIF5B and BNIP-2 form a novel physiological complex in myoblasts and muscle.

To determine whether KIF5B–BNIP-2 interaction was mediated through their direct binding but not by third-party protein(s), we then performed far-Western analysis. Green fluorescent protein (GFP)–KIF5B and GFP-vinculin were transfected into 293T cells and immunoprecipitated with anti–GFP-agarose beads. The isolated GFP-tagged proteins were separated by gel electrophoresis and immobilized on polyvinylidene difluoride (PVDF) membrane. The membranes were probe with purified GST or GST-tagged BNIP-2 protein. Figure 1H shows that GST–BNIP-2 interacts with GFP-KIF5B but not with GFP-vinculin, which was used as negative control. A control Far-western blot did not show binding of GST protein to the GFP-KIF5B or GFP-vinculin (Figure 1H). Therefore we concluded that KIF5B and BNIP-2 interact directly.

Dissecting the critical regions for BNIP-2–KIF5B interaction

We next set out to identify which domain of KIF5B is required for binding to BNIP-2. The amino terminus of KIF5B contains a motor domain for ATP hydrolysis and microtubule binding, whereas the carboxy-terminus tail mediates ATP-independent microtubule binding and regulation of its motor activity (Yang *et al.*, 1989;

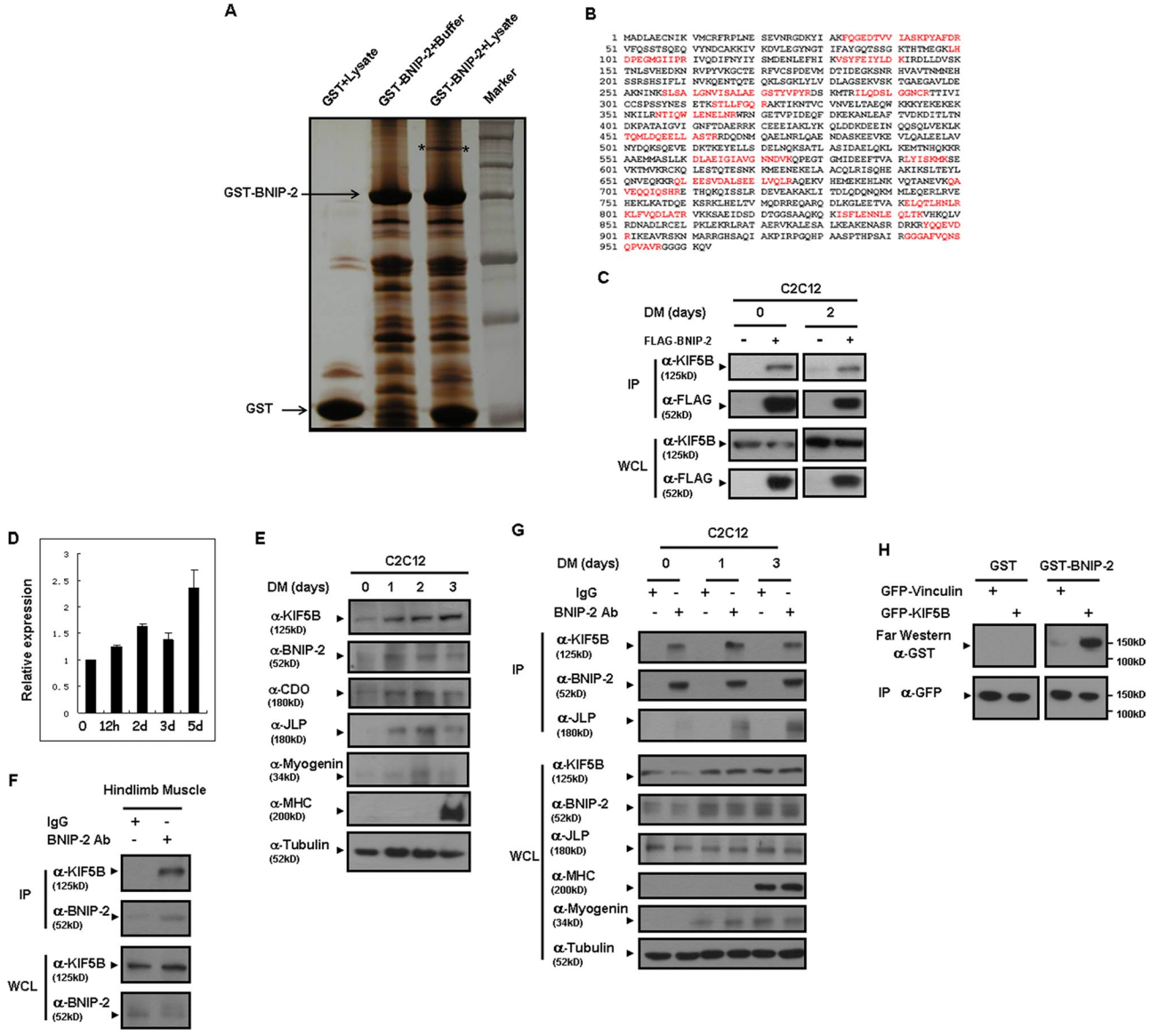

FIGURE 1: KIF5B as a novel binding partner of BNIP-2. (A) A unique band around 125 kDa was found to bind to BNIP-2 (lane 3, asterisks) when comparing the bound proteins on GST or GST recombinant of BNIP-2 (arrow) immobilized on beads after incubation with 293T cell lysate or lysis buffer. (B) The 125-kDa band was subjected to trypsin digestion, followed by MALDI-TOF analysis, and identified as KIF5B. Peptide sequences representing 22% coverage of KIF5B are highlighted in red. (C) C2C12 cells transfected with FLAG–BNIP-2 plasmid proliferated in GM were then transferred to DM for the indicated times. Lysates were immunoprecipitated (IP) with anti-FLAG beads and then Western blotted with KIF5B antibody. (D) Up-regulation of KIF5B expression during C2C12 myoblast differentiation. C2C12 cells were cultured in GM to 80% confluence and then transferred to DM for the indicated times. Cells were subjected to qPCR analysis. KIF5B mRNA levels were significantly increased in differentiating cells (12 h, 2 d , 3 d, and 5 d) compared with undifferentiated cells (0). (E) Lysates of C2C12 cells cultured in GM to 80% confluence and then transferred to DM for the indicated times were subjected to Western blot analysis with the indicated antibodies. (F) Lysates of mouse hindlimb muscle were immunoprecipitated with BNIP-2 antibody and then Western blotted with KIF5B or BNIP-2 antibodies. (G) Lysates of C2C12 cells that were proliferating in GM and then transferred to DM for the indicated times were immunoprecipitated with BNIP-2 antibodies and then Western blotted with KIF5B, BNIP-2, or JLP antibodies. (H) GFP-KIF5B and GFP-vinculin were transfected into 293T cells and immunoprecipitated with anti–GFP-agarose beads (ChromoTek). Isolated GFP-tagged proteins were run on SDS–PAGE gel and immobilized on PVDF membrane. The membranes were probed with purified GST-tagged BNIP-2 protein and detected with rabbit anti-GST, followed by HRP–anti-rabbit. Purified GST was used as control.

Hirokawa *et al.*, 2009). Present between these two domains is a 600–amino acid (aa) region that includes the stalk domain for KIF5B dimerization and light-chain association. A series of KIF5B mutants, as shown in Figure 2A, was prepared and tested for the ability to coimmunoprecipitate HA-tagged BNIP-2. The tail domain and constructs (1–560, 1–370, and 1–446) comprising the motor domain were as effective as the full-length KIF5B in interacting with BNIP-2 (Figure 2B). However, the stalk domain failed to do so. This is consistent with the far-Western analysis showing that both tail and motor domains interact with the GST–BNIP-2 directly

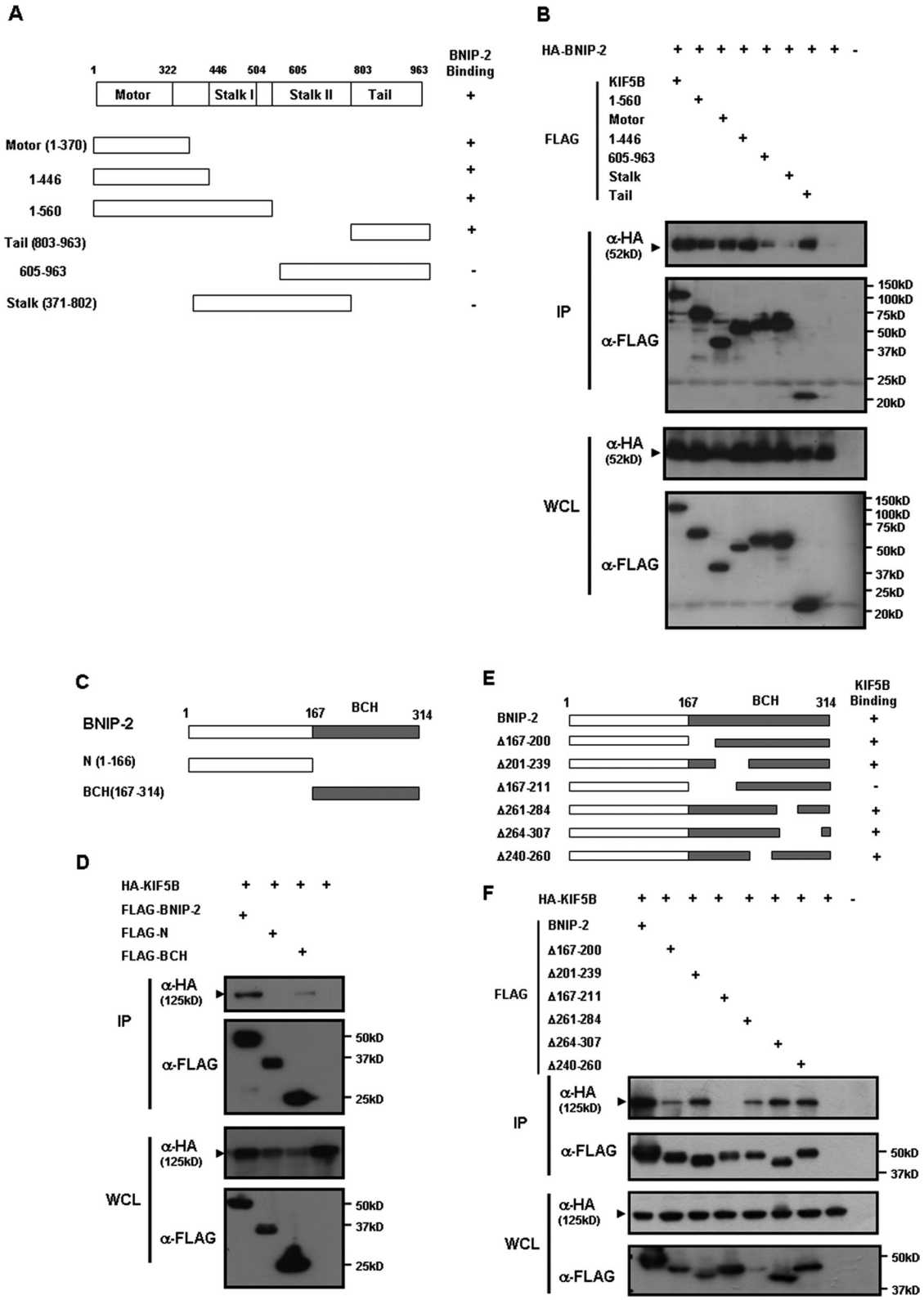

FIGURE 2: Dissecting the critical regions for BNIP-2-KIF5B interaction. (A) Schematic diagram of KIF5B and its mutants and their ability to bind BNIP-2. (B) Lysates of 293T cells transiently transfected with HA-tagged BNIP-2 and FLAG-tagged KIF5B, FLAG-tagged KIF5B mutants, or control (–) expression vectors as indicated were immunoprecipitated (IP) with anti-FLAG beads and then Western blotted with FLAG or HA antibodies. (C) Schematic diagram of BNIP-2 and its mutants. (D) Lysates of 293T cells transiently transfected with HA-tagged KIF5B and FLAG-tagged BNIP-2 or its various mutant expression vectors as indicated were immunoprecipitated with anti-FLAG beads and then Western blotted with FLAG or HA antibodies. (E) Schematic diagram of BNIP-2 and its mutants and their ability to bind KIF5B. (F) Lysates of 293T cells transiently transfected with HA-tagged KIF5B and FLAG-tagged BNIP-2 and its mutants or control (–) expression vectors as indicated were immunoprecipitated with anti-FLAG beads and then Western blotted with FLAG or HA antibodies.

(Supplemental Figure S1B). In addition, FLAG-tagged BNIP-2 could immunoprecipitate both HA-tagged motor and tail, suggesting that the motor and tail domains do not compete with each other for BNIP-2 (Supplemental Figure S1C). Therefore we concluded that KIF5B directly binds BNIP-2 via its motor and tail domains.

The BCH domain is a versatile protein–protein interaction domain (Pan and Low, 2012). We next asked whether this domain on BNIP-2 is critical for targeting KIF5B. A coimmunoprecipitation study showed that the BCH domain, but not the N-terminus of BNIP-2, mediates its interaction with KIF5B (Figure 2, C and D). Further, both motor and tail domains but not the stalk domain could interact with the BCH domain (Supplemental Figure S1D). To further identify the KIF5B binding sites on the BNIP-2 BCH domain, we used BNIP-2 deletion mutants without specific regions of the BCH domain (Figure 2E). These mutants or the wild-type BNIP-2 were coexpressed with HA-KIF5B in cells, and their ability to coimmunoprecipitate was examined. As shown in Figure 2F, the mutant specifically devoid of amino acids 167–211 failed to bind KIF5B, whereas other mutants retained their ability to bind KIF5B. Because both motor and tail domains of KIF5B interact with BNIP-2, we asked whether the 167–211 region is required for targeting the two domains. As shown in Supplemental Figure S2, the deletion construct Δ167–211 binds neither motor nor tail domain. Thus this 45-aa region (167–211) within the BCH domain constitutes a novel KIF5B-binding sequence.

The transport of BNIP-2 is microtubule dependent

KIF5B transports organelles and protein complexes on microtubules (Hirokawa and Noda, 2008). The interaction between KIF5B and BNIP-2 suggests that BNIP-2 could be transported on microtubules. Therefore we detected the endogenous BNIP-2 localization in differentiated myotubes. As shown in Figure 3A, endogenous BNIP-2 was enriched in the protrusion tips of matured myotubes. Consistently, overexpressed BNIP-2 was also concentrated in protrusion regions of both C2C12 myoblast cell (Figure 3B) and differentiated myotubes (Figure 3C), suggesting that the anterograde transport of BNIP-2 in these cells could determine their locality. To monitor the transport of BNIP-2, we used confocal spinning disk microscopy to track GFP-tagged BNIP-2 in live cells. Time-lapse images revealed both anterograde and retrograde transport of BNIP-2–decorated granules in cells, with most of the "BNIP-2–positive" granules actively moving toward the tips of cells (Figure 3D; also see Supplemental Video S1).

To determine whether the transport of BNIP-2 is functionally dependent on microtubules and not simply a diffused complex in the cytosol, we monitored the GFP–BNIP-2 granules in live C2C12 myoblast after treatment with nocodazole, an agent that would interfere with the polymerization of microtubules. As shown in Figure 3E, enrichment of BNIP-2 at the cell protruding ends was blocked by the nocodazole treatment. Consequently, BNIP-2 vesicles were now only seen "oscillating" by time-lapse microscopy analysis (Supplementary Video S2). Coexpression of GFP–BNIP-2 and red fluorescent protein (RFP)–tubulin in C2C12 revealed that the "BNIP-2–positive" granules present precisely on microtubule structures (Figure 3F). Time-lapse analysis of live C2C12 cells showed that GFP–BNIP-2 granules are moving along microtubule filaments (Figure 3G). Taken together, these data demonstrated the microtubule-dependent transport of BNIP-2 toward the tips of cell protrusions.

BNIP-2 is located in endosomal structures

The anterograde transport of BNIP-2 prompted us to further determine the cellular compartments or organelles in which BNIP-2 punctate structures were localized. To this aim, we used a series of organelle markers. Immunofluorescence staining revealed that BNIP-2 does not colocalize with mitochondria (MitoTracker), endoplasm reticulum network (RFP-ER), Golgi, or later endosome (DsRed-Rab7; Supplemental Figure S3). However, the marker for early endosome mRFP-Rab5 displayed significant colocalization with BNIP-2 (Figure 4A, arrowheads and inset). The mRFP-Rab5 displayed similar cellular localization as did endogenous Rab5 (Supplemental Figure S4). To preclude the artifact caused by overexpression of mRFP-Rab5, we stained for endogenous Rab5 or early endosome antigen 1 (EEA1), another marker for early endosome, and confirmed the early endosomal distribution of BNIP-2 (Figure 4, B and C, arrowheads and inset). Their colocalizations were confirmed by quantification analysis (Supplemental Figure S5A). Because early endosomal trafficking is microtubule dependent (Stenmark, 2009), these observations confirm that BNIP-2–positive vesicles are transported along the microtubules. We next examined whether the endosomal distribution of BNIP-2 is BCH domain dependent. We coexpressed full-length BNIP-2 or two mutants lacking or containing the BCH domain (as shown in Figure 2C) with mRFP-Rab5. Immunofluorescence analysis demonstrated that the BCH domain mediates the endosomal distribution of BNIP-2 (Figure 4D and Supplemental Figure S5B).

The anterograde transport of BNIP-2 is dependent on KIF5B

Because the BCH domain is critical for mediating the BNIP-2–KIF5B interaction, we asked whether the anterograde transport of BNIP-2 is dependent on KIF5B. We first monitored fluorescent protein–tagged BNIP-2 and KIF5B in C2C12 myoblast cells. Both GFP–BNIP-2 and RFP-KIF5B can be observed in cell protrusion regions of myoblasts (Figure 5A) and myotubes (Figure 5B). Quantification analysis was performed to confirm their colocalization (Supplemental Figure S5, C and D). By time-lapse imaging analysis, we showed that particles decorated with both proteins moved actively through the live myoblasts (Figure 5C).

To confirm that the anterograde transport of BNIP-2 is indeed a KIF5B-dependent process, we undertook two approaches. First, we asked whether the enrichment of BNIP-2 in cell protrusion regions could be disrupted by the expression of a dominant-negative mutant of KIF5B. Previous studies used KIF tail domains (microtubule-binding domain and portions of the coiled-coil domains deleted) as dominant-negative inhibitors of KIF-dependent vesicle transport (Setou *et al.*, 2002; Jaulin *et al.*, 2007). We thus coexpressed the tail domain of KIF5B together with BNIP-2, followed by immunofluorescence study. As shown in Figure 5D, BNIP-2 was enriched at the cell protrusion tips when cotransfected with FLAG in control C2C12 cells. By contrast, in the presence KIF5B tail domain, a significant pool of BNIP-2 remained at the perinuclear region of the cells, and no protrusion-tip enrichment was observed. Of interest, the motor domain also altered the cellular distribution of BNIP-2, suggesting that the motor–BNIP-2 interaction is also critical for the anterograde transport of BNIP-2 (Figure 5D).

Next, we designed two short interfering RNA (siRNA) sequences targeting KIF5B and assessed the effects of diminished KIF5B level on BNIP-2 trafficking. Each sequence substantially reduced KIF5B protein level in C2C12 myoblasts (Figure 5E). In cells treated with both KIF5B siRNAs, no protrusion-tip localization of BNIP-2 was observed. In contrast, only aberrant aggregation of BNIP-2 in the perinuclear position was detected (Figure 5F). Of interest, the early endosomal localization of BNIP-2 was also disrupted in cells treated with KIF5B siRNA, as shown in Figure 5G (arrows and arrowheads). Thus we confirmed that the anterograde transport of BNIP-2 to cell protrusions requires a functional KIF5B.

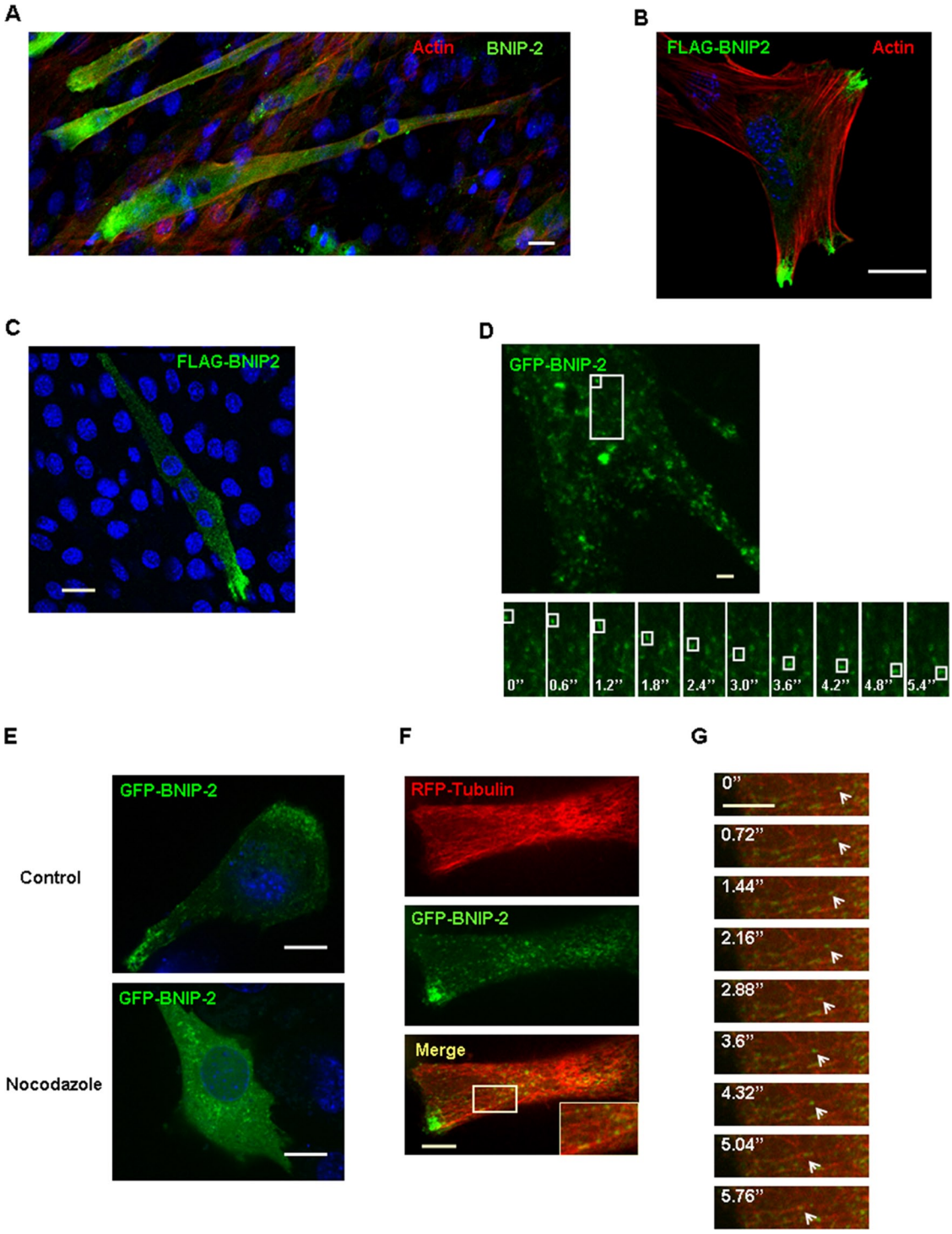

FIGURE 3: Transport of BNIP-2 in cells. (A) C2C12 cells were transferred to DM for 3 d to form myotubes. Myotubes were then fixed and stained for endogenous BNIP-2 as described in *Materials and Methods*. The actin filaments were detected by direct staining with rhodamine-conjugated phalloidin. Bar, 20 μm. (B) C2C12 cells were transfected with plasmids encoding FLAG-BNIP-2. Cells were then fixed and subjected to immunofluorescence study as described in *Materials and Methods*. The actin filaments were detected by direct staining with rhodamine-conjugated phalloidin. Nuclei were visualized by 4′,6-diamidino-2-phenylindole (DAPI) staining of the DNA. Bar, 20 μm. (C) C2C12 cells were transfected with FLAG-BNIP-2 plasmid and transferred to DM for 48 h, followed by immunofluorescence study. Nuclei were visualized by DAPI staining. Bar, 50 μm. (D) C2C12 cells were transfected with GFP–BNIP-2 plasmid and subjected to time-lapse spinning disk microscopy. Bar, 2 μm. (E) C2C12 cells transfected with GFP–BNIP-2 plasmid were incubated for 4 h with dimethyl sulfoxide (control) or nocodazole (20 μM), followed by immunofluorescence analysis. Nuclei were visualized by DAPI staining. Bar, 10 μm. (F) C2C12 cells cotransfected with GFP–BNIP-2 and RFP-tubulin for 36 h and subjected to time-lapse spinning disk microscopy. Bar, 5 μm. (G) Time sequence of BNIP-2–decorated structure (white arrowheads) moving along microtubules. Bar, 5 μm.

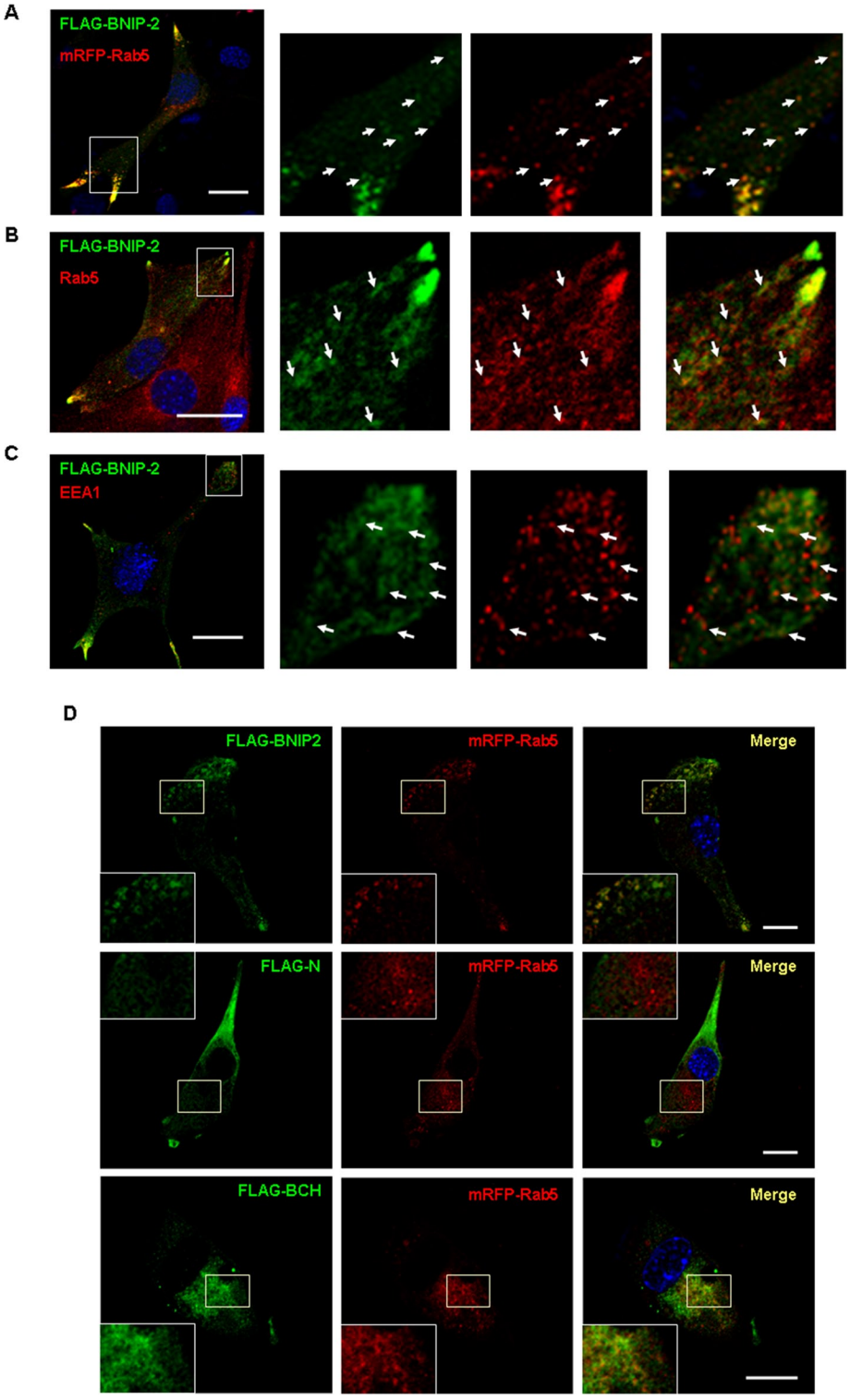

FIGURE 4: Early endosomal localization of BNIP-2. (A) FLAG-tagged BNIP-2 was cotransfected with early endosome marker RFP-Rab5 in C2C12 cells. Cells were then fixed after 24 h and subjected to confocal fluorescence microscopy as described in *Materials and Methods*. Nuclei were visualized by DAPI staining. Bar, 20 μm. (B) C2C12 cells transfected with FLAG–Bnip-2 plasmid for 36 h were fixed and stained for BNIP-2 and endogenous Rab5. Nuclei were visualized by DAPI staining. (C) C2C12 cells transfected with FLAG–Bnip-2 plasmid for 36 h were fixed and stained for BNIP-2 and endogenous EEA1. Nuclei were visualized by DAPI staining. (D) C2C12 cells were cotransfected with mRFP-tagged Rab5 with FLAG-tagged BNIP-2 or its mutants, followed by immunofluorescence study as described in *Materials and Methods*. Nuclei were visualized by DAPI staining. Bar, 20 μm.

KIF5B positively modulates myogenic differentiation and p38MAPK activation

BNIP-2 was previously shown to be involved in promoting myogenesis (Kang *et al.*, 2008). Our finding that KIF5B is required for anterograde transport of BNIP-2 suggests that KIF5B could be promyogenic. To test this hypothesis, we examined the differentiation of C2C12 myoblasts with diminished or enhanced KIF5B level by KIF5B siRNA or stable expression. We treated C2C12 with KIF5B siRNA and showed that these cells had substantially reduced KIF5B expression (Figure 6A). The depletion of KIF5B results in a smaller percentage of cells with differentiation marker myosin heavy chain (MHC) expression by immunofluorescence analysis (Figure 6B). C2C12 cells that were treated with each KIF5B siRNA were shorter and contained fewer nuclei in MHC-positive myotubes than control cells transfected with an irrelevant siRNA sequence (Figure 6, B and C). Western blot confirmed that the expression of MHC was much reduced by KIF5B siRNA (Figure 6D). We next examined the effects of overexpression of KIF5B on myogenesis. Stable expression of FLAG-tagged KIF5B resulted in a modest increase of KIF5B by about threefold (Figure 7A). Control and KIF5B-expressing cells were then triggered to differentiation for 2 d. Compared to negative control, KIF5B-expressing cells displayed enhanced levels of MHC by immunofluorescence analysis (Figure 7B). MHC-positive myotubes in KIF5B expression C2C12 cells contained a greater fraction of cell nuclei (Figure 7C). Further, Western blot experiments showed that expression of both MHC and myogenin is accelerated and enhanced (Figure 7D). Thus we concluded that KIF5B is critical for myoblast differentiation.

BNIP-2 regulates myogenesis by activating p38MAPK (Kang *et al.*, 2008). Because JLP, the scaffold protein for p38MAPK and MKK3/6, could be immunoprecipitated by BNIP-2 (Figure 1G), we tested whether BNIP-2 also interacts with p38MAPK and MKKs. As shown in Figure 8A, HA-tagged BNIP-2 could be immunoprecipitated by FLAG-tagged p38MAPK, MKK3, or MKK6. Further, FLAG-tagged p38MAPK, MKK3, or MKK6 could interact with the endogenous BNIP-2 in C2C12 myoblasts (Figure 8B), confirming the protein complex formed by BNIP-2, p38MAPK, and MKK3/6. Thus our finding that KIF5B is critical for BNIP-2 trafficking suggests that KIF5B could be involved in regulating p38MAPK activity. This possibility was tested by reducing or enhancing KIF5B level and detecting the phosphorylated form of p38MAPK (pp38). We first

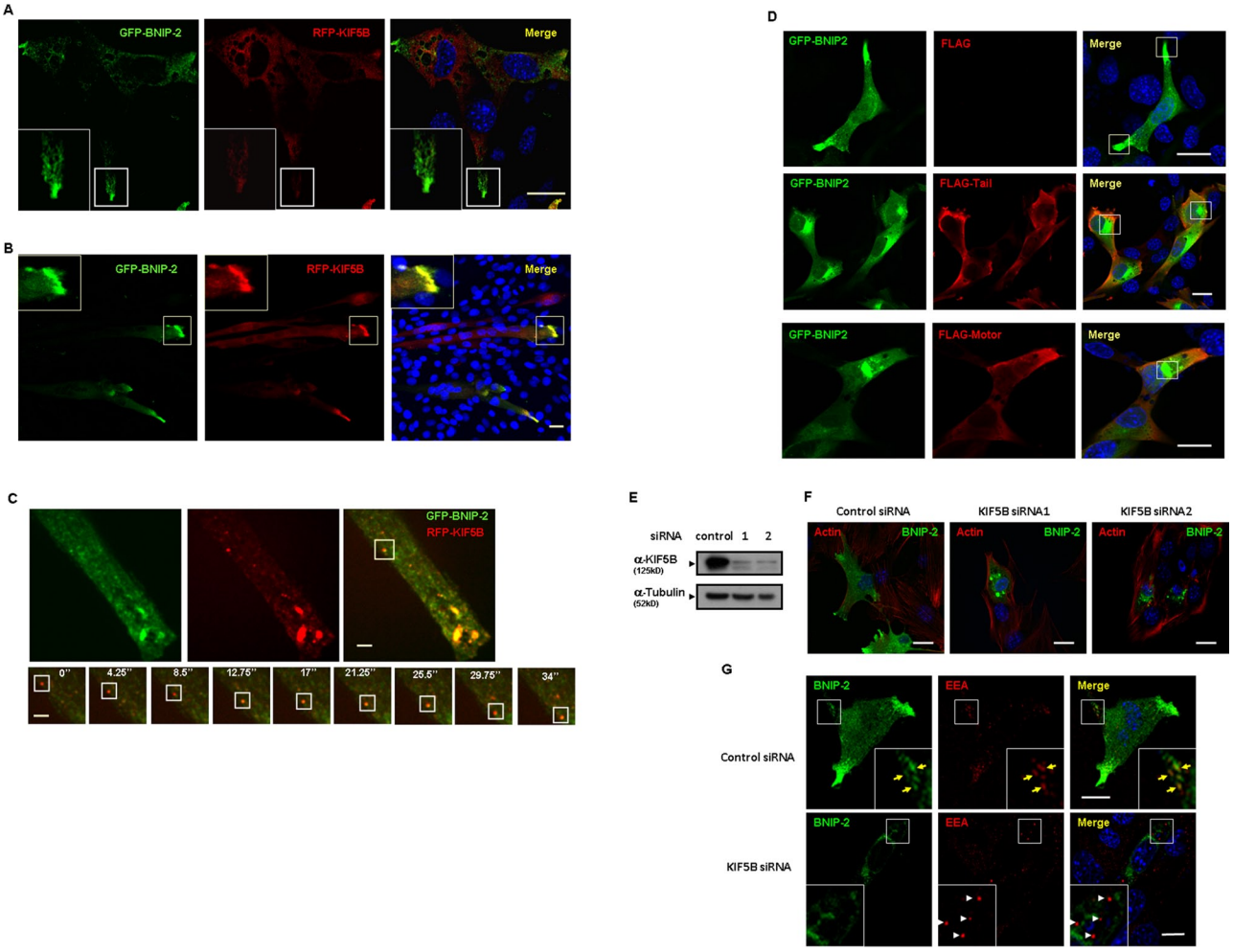

FIGURE 5: The anterograde transport of BNIP-2 is dependent on KIF5B. (A) C2C12 cells cultured in growth medium were cotransfected with GFP–BNIP-2 and RFP-KIF5B plasmids, followed by confocal fluorescence microscopy analysis. Nuclei were visualized by DAPI staining. Bar, 20 μm. (B) C2C12 cells were cotransfected with GFP–BNIP-2 and RFP-KIF5B plasmids for 24 h and transferred to differentiation medium for 72 h. Cells were fixed and subjected to Olympus FV1000 confocal fluorescence microscopy. Nuclei were visualized by DAPI staining. Bar, 20 μm. (C) C2C12 cells were cotransfected with GFP–BNIP-2 and RFP-KIF5B plasmids for 24 h and subjected to time-lapse spinning disk microscopy. Bar, 2 μm. (D) GFP–BNIP-2 was cotransfected with pXJ40-FLAG vector (control), FLAG-KIF5B tail domain, or motor domain in C2C12 cells for 36 h. Cells were fixed and subjected to immunofluorescence study. Nuclei were visualized by DAPI staining. Bar, 20 μm. (E) Lysates of C2C12 cells transfected with two independent KIF5B siRNA sequences (designated 1 and 2) or control siRNA sequence (control) were Western blotted with KIF5B or tubulin antibodies as control. (F) C2C12 cells transfected with control siRNA or KIF5B siRNA for 48 h, followed by transfection with GFP–BNIP-2 for 36 h. Cells were fixed and subjected to immunofluorescence analysis. The actin filaments were detected by direct staining with rhodamine-conjugated phalloidin. Nuclei were visualized by DAPI staining. Bar, 20 μm. (G) C2C12 cells transfected with control siRNA or KIF5B siRNA for 48 h, followed by transfection with GFP–BNIP-2 for 36 h. Cells were fixed and stained for endogenous EEA1, followed by immunofluorescence analysis. Nuclei were visualized by DAPI staining. Bar, 20 μm.

transfected cells with KIF5B siRNA and detected the p38MAPK activity before and after differentiation. As shown in Figure 8C, KIF5B knockdown decreased the active form of p38MAPK in myoblasts in growth and differentiation media. Consistently, stably overexpressing KIF5B in C2C12 resulted in higher levels of phosphorylated p38MAPK (Figure 8D). These data indicated that KIF5B is involved in p38MAPK activation during myogenesis.

KIF5B-dependent transport is critical for the promyogenic effect of BNIP-2

Our finding showed that KIF5B, the novel interacting partner of BNIP-2, is important for p38MAPK activation and myoblast differentiation. This prompted us to ask whether the KIF5B-dependent transport and localization was indeed critical for the promyogenic effects of BNIP-2. We tested this hypothesis by three separate approaches. The BNIP-2 Δ167-211 mutant does not bind KIF5B or its motor or tail domain (Figure 2F and Supplemental Figure S2). We first examined the ability of this mutant to promote myotube formation by stably transfecting it into C2C12 and then measuring expression of MHC and myogenin. As shown in Figure 9A, expression of wild-type BNIP-2 stimulated MHC expression and production of multinucleated myotubes. In contrast, the Δ167–211 mutant stable cell line lost the ability to enhance MHC and myogenin expression. Further, Δ167–211 stable myoblasts differentiated fewer MHC-positive myotubes, and these myotubes were shorter and contained fewer nuclei (Figure 9, B and C).

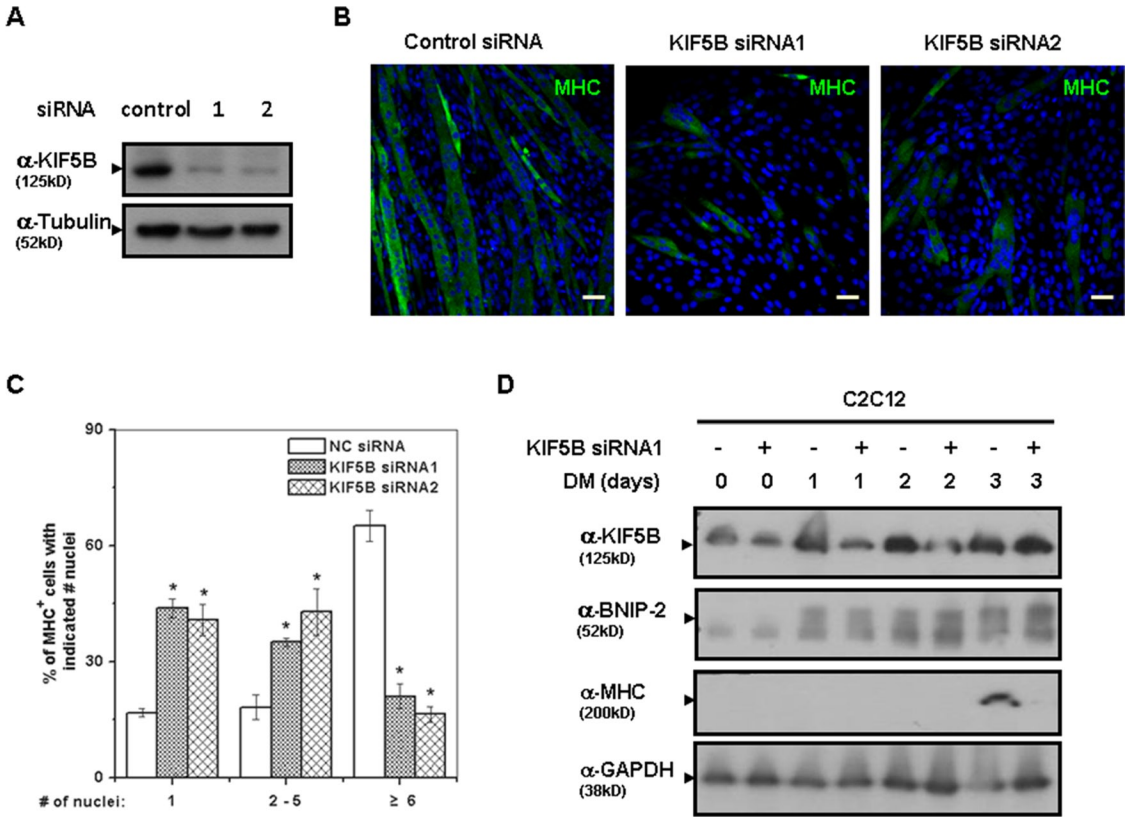

FIGURE 6: Knockdown of KIF5B reduces myogenic differentiation. (A) Lysates of C2C12 cells transfected with two independent KIF5B siRNA sequences (designated 1 and 2) or control siRNA sequence (control) were Western blotted with KIF5B or tubulin antibodies as control. (B) C2C12 cells that transfected with KIF5B siRNA sequences or an irrelevant (control) sequence were cultured in DM, fixed, and stained with MHC antibody and DAPI for immunofluorescence analysis. Bar, 50 μm. (C) Quantification of myotube formation by C2C12 cells transfected with siRNAs shown in B. Data are means ± SD ($n = 3$). Significant difference from control, *$p < 0.01$. (D) C2C12 cells transfected with control or KIF5B siRNA were cultured in GM (0) or in DM for the indicated times, followed by Western blot analysis of KIF5B, BNIP-2, MHC, and glyceraldehyde-3-phosphate dehydrogenase proteins.

Because both motor and tail domains of KIF5B could abolish the localization of BNIP-2 at cell protrusions (Figure 5D), we next asked whether these two domains could inhibit myogenesis. We stably overexpressed motor and tail domains in C2C12 cells. In both cases, they resulted in delayed induction of the differentiation markers myogenin and MHC (Figure 9D).

Finally, we tested whether the promyogenic effect of BNIP-2 could be demolished by depleting KIF5B. C2C12 cells that were stably overexpressing BNIP-2 displayed elevated levels of MHC and myogenin relative to vector control cells, whereas transfection of KIF5B siRNA largely prevented the BNIP-2–induced increase in these differentiation markers (Figure 9E). Thus it can be concluded that KIF5B-dependent transport is indeed critical for BNIP-2 to trigger downstream signals leading to myogenesis.

DISCUSSION

Cell–cell interaction of precursor myoblasts is critical for activating the essential p38MAPK promyogenic signaling pathways (Krauss *et al.*, 2005). Previous studies reveal a cell surface complex for p38MAPK activation that includes the Cdo receptor, scaffold proteins JLP and BNIP-2, MKK3/6, and p38MAPK (Kang *et al.*, 1998, 2002, 2008; Takaesu *et al.*, 2006). However, the mechanism for activating Cdo pathway at the appropriate subcellular location and time during myogenesis is not well understood. In this article, we describe the identification of the motor protein KIF5B as a novel interacting partner of BNIP-2. KIF5B is critical for p38MAPK activation and myoblast differentiation via transporting BNIP-2, revealing the spatial regulation of Cdo pathway during myogenesis.

Transportation of scaffold protein by kinesin

Scaffold proteins play important roles for precise regulation of MAPK signaling by organizing MAPK modules and thus preventing inappropriate activation from irrelevant stimuli (Harding *et al.*, 2005; Good *et al.*, 2011; Pan *et al.*, 2012). Studies further revealed that subcellular translocation of scaffold proteins is critical for temporal-spatial regulation of MAPK signaling and differentiation (Harding *et al.*, 2005; Bracale *et al.*, 2007; Aoyama *et al.*, 2009). This regulation apparently relies on kinesin-1–mediated intracellular transport, since an increasing number of signaling proteins have been identified to be linked to kinesin-1 (Setou *et al.*, 2002; Glater *et al.*, 2006; Blasius *et al.*, 2007; Cho *et al.*, 2007; Sun *et al.*, 2011). Activation of p38MAPK is critical for myogenic differentiation (Puri *et al.*, 2000; Wu *et al.*, 2000; de Angelis *et al.*, 2005). It was previously reported that the cell surface receptor Cdo interacts with scaffold proteins JLP and BNIP-2, which subsequently activate p38MAPK during myogenic differentiation (Kang *et al.*, 2008). However, the spatial-temporal regulation of this Cdo-p38MAPK pathway is far from clear. Here we demonstrated that scaffold protein BNIP-2 binds KIF5B, the ubiquitously expressed kinesin heavy-chain isoform, and is transported in a KHC-dependent manner. Therefore we find a previously unknown link between the Cdo signaling pathway and the kinesin-1 transportation system. Of interest, it was previously shown that

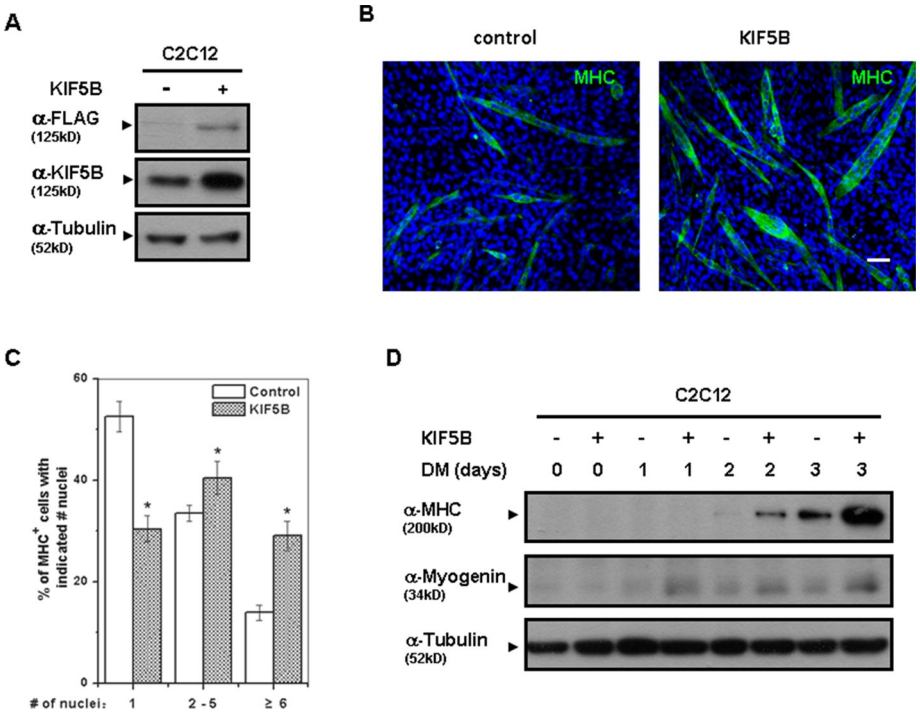

FIGURE 7: Stable overexpression of KIF5B enhances myogenic differentiation. (A) Lysates of C2C12 cells stably transfected with a control pXJ40-GFP plasmid (–) or with expression plasmid harboring FLAG-tagged KIF5B cDNA as indicated (+) were Western blotted with FLAG or KIF5B antibodies. (B) C2C12 cells stably transfected with FLAG-tagged KIF5B or control GFP plasmids were cultured in DM for 48 h. Cell then were fixed and stained with MHC antibody, followed by DAPI stain for confocal fluorescence microscopy. Bar, 50 μm. (C) Quantification of myotube formation by cell lines shown in B. Data are means ± SD ($n = 3$). Significant difference from control, *$p < 0.01$. (D) Western blot analysis of muscle-specific proteins (MHC and myogenin) by C2C12 cell transfectants cultured in GM (0) or in DM for the indicated times. Western blot of tubulin is a loading control.

BNIP-H/caytaxin, the neuronal BNIP-2 family member, is transported in neurons by interacting with KLC1 (Aoyama *et al.*, 2009), However, our data show that KHC is involved in mediating anterograde transport of BNIP-2 in myoblasts. Such variation in motor recognition is likely due to different cell types and subcellular environments, details of which await further investigation.

KHC is structured into three functional domains—the N-terminal motor domain, the C-terminal tail domain, and a stalk domain that spans the other two (Yang *et al.*, 1989; Hirokawa and Noda, 2008; Hirokawa *et al.*, 2009). The stalk domain is responsible for KHC dimerization and KLC association, and the tail is important for cargo recognition and motor activity modulation (Hirokawa *et al.*, 1989, 2009). Of interest, in strong contrast to other KHC-interacting proteins, BNIP-2 binds to both the motor and tail domains of KHC through its BCH domain. It is conceivable that the BNIP-2–tail interaction is critical for BNIP-2 trafficking, since the tail governs the cargo recognition. However, there remains the question of the significance of the interaction between BNIP-2 and the motor domain. This is of interest since the motor domain has very few interacting partners other than tubulin. It is well documented that the motor and tail domains of KHC form an intramolecular interaction when not activated (Hirokawa *et al.*, 2009; Verhey and Hammond, 2009). Further, previous study showed that cargo binding to the tail domain may not be sufficient for kinesin activation (Wozniak *et al.*, 2006). In this regard, it is possible that there exist two pools of BNIP-2 for targeting KIF5B. One pool of BNIP-2 interacts with the motor domain to ensure the activation of KHC, whereas the other pool of BNIP-2 interacts with the tail domain for its transportation. Both modes of interaction are important since either motor or tail domain could disrupt the anterograde transport of BNIP-2 and inhibit myoblast differentiation (Figures 5D and 9D). This is in line with the finding that motor and tail domains do not compete with each other for BNIP-2 (Supplemental Figure S1C). The precise mechanism by which BNIP-2 binds to KHC awaits further biophysical and structural investigation.

Roles of KHC in myogenesis

Myogenesis is a dynamic fusion process in which myoblasts withdraw from the cell cycle and finally fuse to form mature muscle fiber (Buckingham, 2006; Rochlin *et al.*, 2010; Abmayr and Pavlath, 2012). This is a multistage process that starts from the specification of uncommitted precursor cells and is followed by cell elongation, alignment, and fusion (Krauss *et al.*, 2005). It is believed that these stages are under tight control of various transcription factors and distinct signaling pathways (Krauss *et al.*, 2005; Knight and Kothary, 2011). Previous studies revealed the roles of kinesin in neuronal differentiation (Bracale *et al.*, 2007). Because microtubule inhibitors inhibit myotube formation, it was proposed that motor proteins might be involved in myogenesis regulation (Siebrands *et al.*, 2004). Recent reports revealed the essential roles of KIF5B in proper nuclear positioning during the forming of myotubes (Metzger *et al.*, 2012; Wilson and Holzbaur, 2012; Folker *et al.*, 2014). Here we demonstrated that KIF5B is involved in early differentiation, since knockdown of KIF5B reduced the expression of myogenin. Further, loss- and gain-of function experiments in myoblasts indicated that KHC regulates p38MAPK activity that is critical for triggering the activation of myogenic transcription factors. All these findings highlight the emerging role of KIF5B as an important regulator of myogenesis.

The diverse roles of KIF5B in regulating myogenic differentiation are mediated by interacting with and transporting different scaffold or adaptor proteins. For example, KIF5B localizes to myonuclei by interacting with MAP7 to promote nuclear positioning in *Drosophila* embryos (Metzger *et al.*, 2012). In developing C2C12 cells, the Klarsicht/ANC-1/Syne homology (KASH) protein links kinesin-1 to the nuclear surface for maintaining appropriate nuclei distribution (Wilson and Holzbaur, 2012). Furthermore, it was recently found that KIF5B transports desmin, α-sarcomeric actin, and nestin to the growing tips of the elongating myotubes (Wang *et al.*, 2013). Here we demonstrated that KIF5B is essential for transporting BNIP-2, a critical signaling scaffold protein of the Cdo pathway, in myoblasts and myotubes. There is still much to be elucidated on the mechanism by which these interactions are regulated.

Distinct subcellular compartment of BCH domain–containing proteins

We recently established the roles of the BCH domain in modulating a variety of cellular events (Pan and Low, 2012; Ravichandran and Low, 2013). Of interest, these BCH domain–containing proteins

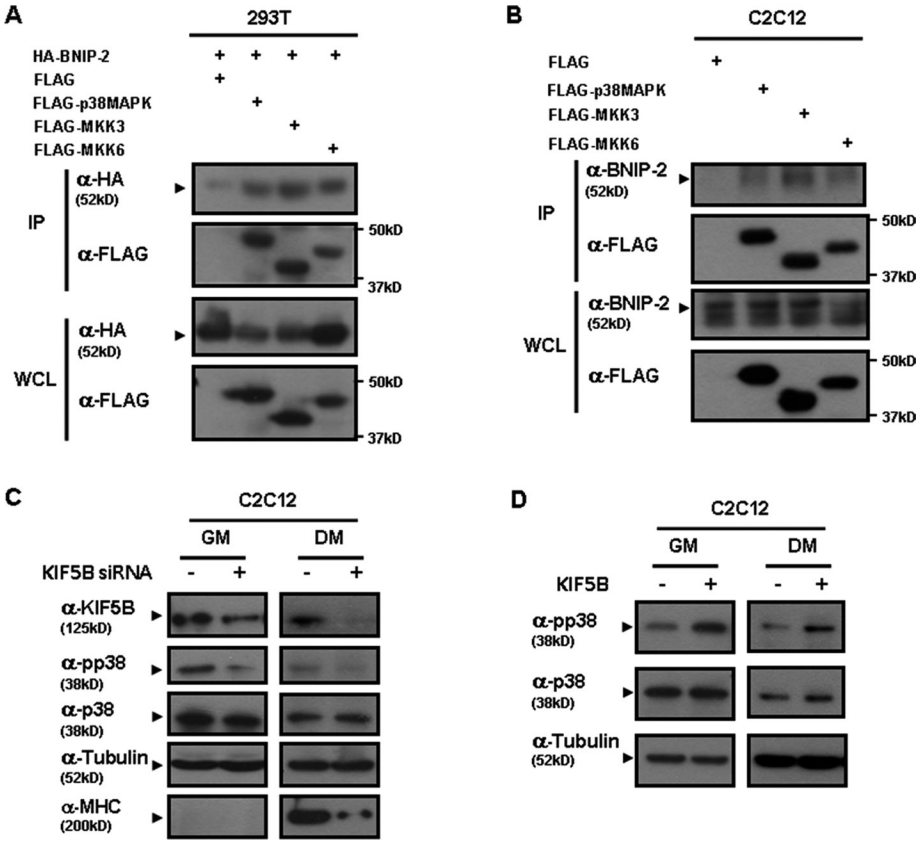

FIGURE 8: KIF5B is required for p38MAPK activation. (A) HA-tagged BNIP-2 was cotransfected with FLAG-tagged-p38MAPK, MKK3, MKK6, or vector control in 293T cells. Lysates were immunoprecipitated with anti-FLAG beads and then Western blotted with FLAG or HA antibodies. (B) Lysates of C2C12 cells transfected with FLAG-tagged p38MAPK, MKK3, MKK6, or vector control were immunoprecipitated with anti-FLAG beads and then Western blotted with BNIP-2 or FLAG antibodies. (C) Lysates of C2C12 cells transfected with KIF5B siRNA (+) or control siRNA (–) in GM or cultured for 48 h in DM were Western blotted with anti–phospho-p38MAPK (pp38) or p38MAPK (p38) antibodies. (D) Lysates of C2C12 cells stably expressing KIF5B (+) or control GFP plasmid (–) in GM or cultured for 48 h in DM were Western blotted with pp38 or p38 antibodies.

display distinct subcellular localizations. BNIP-H (caytaxin) translocates mitochondria at neurite termini, and p50RhoGAP decorates early and later endosomes (Sirokmany *et al.*, 2006; Aoyama *et al.*, 2009). Here we showed that BNIP-2 is localized to Rab5- and EEA-positive endosomes via its BCH domain (Figure 4). The significance of the endosomal localization of BNIP-2 remains to be seen. Endosomes provide crucial platforms for the assembly of specific signaling complexes and anterograde transport of endosomal localized signaling complexes that are important for diverse cellular functions (Miaczynska and Bar-Sagi, 2010). For example, Arf6-dependent anterograde transport localized Cdc42-βPIX protein complex to the cell leading edge, whereas Rab5-activated Rac was delivered to plasma membrane during cell migration (Palamidessi *et al.*, 2008; Osmani *et al.*, 2010). Similar to the case of neurons, signals travel for long distance to reach the plasma membrane in myotubes. Instead of diffusion, targeted delivery of BNIP-2 by KIF5B-dependent anterograde transport ensures that BNIP-2 is properly regulated in space and time to control myogenic signaling.

In relation to its targeting, it would be interesting to see how the specificity for the endosomal compartmentalization of BNIP-2 can be achieved. Rab GTPases that regulate budding, trafficking, and fusion of endocytic vesicles at the different compartments could be candidates (Stenmark, 2009). This speculation is based on the previous finding that the endosomal localization of p50RhoGAP relies on its targeting to Rab5 and Rab11 (Sirokmany *et al.*, 2006). Our data showed that BNIP-2 not only colocalizes with Rab5-positive vesicles, it also induces Rab5 enrichment in the cell protrusion end. This suggests that BNIP-2 might play a role in recycling Rab5-positive vesicles and further raises the possibility and Rab5 might be involved in myoblast differentiation. Further investigation on this issue is underway.

Taken together, our work demonstrates the importance of KIF5B in mediating the transport of scaffold protein BNIP-2 and regulating p38MAPK activity during myogenic differentiation. This finding not only sheds light on the increasing evidence that intracellular trafficking is critical for myogenesis, but it also identifies BNIP-2 as one of the key missing links in this process, thus adding to the versatility of this scaffold protein in regulating cell dynamics and signaling.

MATERIALS AND METHODS

Cell culture and transfection

C2C12 cells were grown in DMEM (high glucose) supplemented with 15% (vol/vol) fetal bovine serum (FBS), and human 293T cells were grown in RPMI 1640 medium supplemented with 10% (vol/vol) FBS, 2 mM L-glutamine, 100 U/ml penicillin, and 100 mg/ml streptomycin (all from Hyclone Laboratories, Logan, UT). Cells in six-well plates were transfected with TransIT-LT1 (Mirus Bio, Madison, WI) or Lipofectamine 2000 (Invitrogen, Carlsbad, CA) according to the manufacturer's protocol.

Antibodies

Antibodies used were the following: anti-EEA1 (#3288; Cell Signaling Technology, Danvers, MA), anti-Rab5 (#3547; Cell Signaling Technology), anti-p38MAPK (sc-7972; Santa Cruz Biotechnology, Dallas, TX), anti-pp38MAPK (#4511; Cell Signaling Technology), anti-MHC (MF-20; Developmental Studies Hybridoma Bank, Iowa City, IA), anti-myogenin (F5D; Developmental Studies Hybridoma Bank), anti-Bnip-2 (H-126; Santa Cruz Biotechnology), anti-KIF5B (ab42492; Abcam, Cambridge, MA), anti-JLP (ab12331; Abcam), anti-CDO (R&D systems), anti-FLAG epitope (F7425; Sigma-Aldrich, St. Louis, MO), anti-HA epitope (715500; Invitrogen), and anti-tubulin (M1301-3; HuaAn Biotechnology, Hangzhou, China).

Identification of BNIP-2 interaction partners

Cells were lysed in lysis buffer (50 mM 4-(2-hydroxyethyl)-1-piperazineethanesulfonic acid, pH 7.4, 150 mM sodium chloride, 1.5 mM magnesium chloride, 5 mM EDTA, 10% [vol/vol] glycerol, 1% [vol/vol] Triton X-100, and a mixture of protease inhibitors [Roche Diagnostics, Indianapolis, IN]), 5 mM sodium orthovanadate, and 25 mM glycerol phosphate (Sigma-Aldrich, St. Louis, MO). The GST–BNIP-2 proteins, coupled to glutathione beads, were incubated with precleared cell lysates. The bound proteins

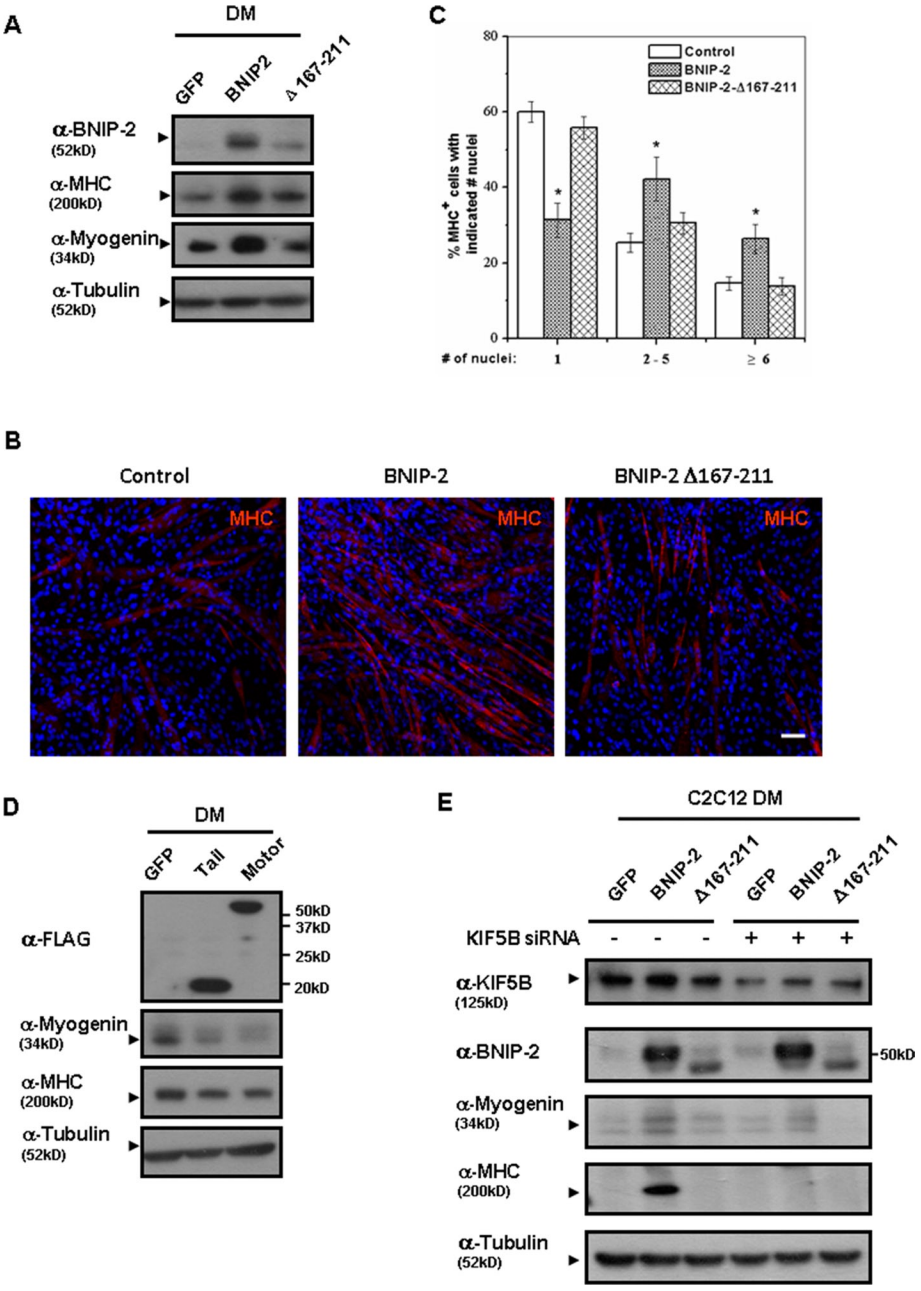

FIGURE 9: KIF5B-dependent transport is critical for the promyogenic effect of BNIP-2. (A) C2C12 cells stably transfected with a control pXJ40-GFP plasmid, expression plasmid harboring FLAG-tagged BNIP-2, or FLAG-tagged BNIP-2 Δ167-211 mutant were cultured in DM for 48 h. Cell lysates were Western blotted with BNIP-2, MHC, or myogenin antibodies. Western blot of tubulin is loading control. (B) C2C12 cells stably transfected with FLAG-tagged KIF5B, FLAG-tagged BNIP-2 Δ167-211 mutant, or control GFP plasmids were cultured in DM for 48 h. Cells then were fixed and stained with MHC antibody, followed by DAPI stain for confocal fluorescence microscopy. Bar, 50 μm. (C) Quantification of myotube formation by cell lines shown in B. Data are means ± SD ($n = 3$). Significant difference from control, *$p < 0.01$. (D) C2C12 cells stably transfected with a control pXJ40-GFP plasmid, FLAG-tagged tail, or FLAG-tagged motor mutant were cultured in DM for 48 h. Cell lysates were Western blotted with BNIP-2, MHC, or myogenin antibodies. Western blot of tubulin is loading control. (E) C2C12 cells stably transfected with a control pXJ40-GFP plasmid, FLAG-tagged BNIP-2, or FLAG-tagged BNIP-2 Δ167-211 mutant were treated with KIF5B siRNA sequences (+) or an irrelevant sequence (–). Cells were then cultured in DM for 48 h, and lysates were Western blotted with the indicated antibodies.

were resolved by SDS–PAGE and visualized by silver staining (Bio-Rad, Hercules, CA). The unique bands were excised and digested with trypsin. Mass spectra were acquired with a MALDI-TOF mass spectrometer (Voyager STR BioSpectrometry work station; Applied Biosystems) operating in the delayed-extraction reflectron mode. Peptide mass fingerprints of the tryptic peptides from MALDI-TOF mass spectrometric data were used to search the National Center for Biotechnology Information protein database with the programs MS-Fit (http://prospector.ucsf.edu/prospector/mshome.htm) and Mascotsearch engine (www.matrixscience.com).

Real-time qPCR

Total RNA was extracted with RNeasy Kit (Qiagen, Chatsworth, CA). Reverse transcription was performed with SuperScript III reverse transcriptase kit (Invitrogen). cDNA was quantified by real-time qPCR using KAPA SYBR FAST qPCR MasterMix kit (Kapabiosystems, Wilmington, MA) and the real-time PCR system (Applied Biosystems, Foster City, CA).

Purification of GST-tagged fusion proteins

The cDNA encoding the proteins of interest were cloned into the pGEX4T1 vector (Amersham Pharmacia Biosciences, Piscataway, NJ) for production of GST fusion proteins. The constructs were subsequently transformed into *Escherichia coli* BL21 LysS cells. A single colony was picked in LB medium containing ampicillin and grown at 37°C to OD_{600} 0.3–0.6. Isopropyl-β-D-thiogalactoside, 1 mM, was added for induction at 37°C. The induced cells were collected by centrifugation and resuspended in 5 ml lysis buffer (1× phosphate-buffered saline [PBS], 1% Triton-X, 1.52% dithiothreitol [wt/vol]), and Complete proteinase inhibitor (Roche Molecular Biochemicals, Indianapolis, IN) and then applied for sonication. The sonicated cell lysates were centrifuged, and the supernatants were collected and incubated with glutathione-Sepharose beads (GE Healthcare Bio-Sciences, Pittsburgh, PA) for 1 h at 4°C to acquire GST fusion proteins. Sepharose bead–bound GST-fusion proteins were eluted with 20 mM reduced glutathione (Sigma-Aldrich) in PBS.

RNA interference

C2C12 myoblasts at 30–40% confluency were transfected with 100 nM siRNA using Lipofectamine RNAiMAX (Invitrogen) according to the manufacturer's protocol. Sequences of siRNAs were siKIF5B1, 5′-GAGAUGAAGUGGAGGCAAA-3′; and siKIF5B2, 5′-GCACACAGACUGAGAGCAA-3′. The sequence of control siRNA was 5′-UUCUCCGAACGUGUCACGU-3′.

Construction of expression plasmids

Full-length cDNA of KIF5B was cloned into a HA-, GFP-, and FLAG-tagged expression vector, pXJ40 (E. Manser, Institute of Molecular and Cell Biology, Singapore). Constructions used in the cellular localization study were DsRed-ER (Clontech), pEYFP-Golgi (#6909-1; Clontech), mRFP-Rab5 (Vonderheit and Helenius, 2005; #14437; Addgene), and DsRed-Rab7 (Choudhury *et al.*, 2002; #12661; Addgene). Deletion mutants were generated by PCR using specific primers facilitated by restriction sites. For each construct, several clones were chosen and sequenced to entirety in both directions to confirm their identity. All plasmids were purified using Axygen miniprep kit for use in transfection experiments. *E. coli* strain DH5α was used as host for propagation of the clones.

Immunoprecipitation studies and Western blot analyses

Control cells or cells transfected with expression plasmids were lysed in lysis buffer (150 mM sodium chloride, 50 mM Tris, pH 7.3, 0.25 mM EDTA, 1% [wt/vol] sodium deoxycholate, 1% [vol/vol] Triton X-100, 0.2% sodium fluoride, 0.1% sodium orthovanadate, and a mixture of protease inhibitors from Roche Applied Science, Indianapolis, IN). Lysates were immunoprecipitated (IP) with anti-FLAG M2 beads (Sigma-Aldrich) and the associated proteins separated on SDS–PAGE and probed with anti-HA (for cotransfection experiments) or other indicated antibodies. Five percent of total cell lysates were run in SDS/PAGE gels and analyzed by immunoblotting with anti-HA (Zymed), anti-FLAG (Sigma-Aldrich), or indicated antibodies. For immunoblotting analysis of dissected hindlimbs, hindlimb muscles from mice were pulverized and solubilized with lysis buffer. Lysates were then analyzed by immunoblotting for the indicated antibodies.

Direct binding assay by far-Western GST–protein–protein interaction

We subjected 293T lysates transfected with GFP- or FLAG-tagged expression plasmids to immunoprecipitation with anti-GFP-agarose beads (ChromoTek, Hauppauge, NY) or anti-FLAG M2 affinity gel. Immunoprecipitated proteins were separated by SDS–PAGE and transferred to PVDF membrane. After blocking, the membranes were incubated with 5 μg/ml purified GST or GST-BNIP-2 in PBS supplemented with 3% bovine serum albumin. The membranes were then washed, followed by probing with rabbit anti-GST. After primary antibodies incubation, the blots were washed and probed with goat anti-rabbit conjugated with horseradish peroxidase (HRP; Sigma-Aldrich). Signals were detected by exposure to x-ray film (Fuji Photo Film, Tokyo, Japan). The blots were then stripped with stripping buffer (25 mM glycine, pH 2, with 1% [wt/vol] SDS) and reprobed with rabbit anti-FLAG or anti-GFP.

Myoblast differentiation

To induce differentiation of C2C12 cells, cultures were transferred from DMEM containing 15% FBS (GM) to DMEM containing 2% horse serum (DM). Myotube formation in stable and transient assays was performed and quantified as previously described (Kang *et al.*, 2008). Statistical analysis of the number of nuclei in MHC+ versus MHC– cells was done with Student's *t* test.

Stable overexpression studies in myoblasts

For stable overexpression studies in myoblasts, pXJ40 vectors encoding FLAG-tagged forms of Bnip-2 (Low *et al.*, 1999, 2000) or KIF5B were cotransfected with pBabePuro into C2C12 cells with Lipofectamine 2000, and cultures were selected in puromycin-containing medium. Drug-resistant cells were pooled and analyzed. Multiple such pools were studied in each case.

Immunofluorescence and direct fluorescence studies

Cells were seeded on coverslips in a six-well plate and transfected with various expression constructs for 24–36 h and then stained for immunofluorescence detection using confocal fluorescence microscopy or directly visualized for cells expressing GFP-tagged proteins as previously described (Zhou *et al.*, 2002). FLAG-tagged proteins were detected with monoclonal anti-FLAG followed by Texas red– or fluorescein isothiocyanate dye–conjugated goat anti-mouse IgG (Invitrogen). Filamentous actin was detected by rhodamine–phalloidin (Molecular Probes), and microtubules were detected by anti-tubulin (Sigma-Aldrich), followed by Alexa Fluor 488–conjugated goat anti-mouse IgG (Invitrogen). The images were collected with a 63×/1.4 numerical aperture or 20× objective lens using appropriate laser excitation on a LSM510 Meta laser-scanning confocal microscope (Carl Zeiss) or an Olympus IX81-FV1000 laser-scanning confocal microscope. The detector gain was first optimized by sampling various regions of the coverslip and then fixed for each specified channel. Once set, the detector gain value was kept constant throughout the image acquisition process. Images were analyzed with Zeiss LSM Image Examiner Software or FV10-ASW 3.0 Viewer. For live-cell imaging, cells in chambers were imaged in medium on an incubator to maintain cultures at 37°C and 5% CO_2. Images were captured with Olympus UplanFLN 100×O PH objective lens and a charge-coupled device camera (ANDOR DU-897D) using a fluorescence microscope (Olympus IX81). Images were analyzed with MetaMorph 7.7.8 software.

ACKNOWLEDGMENTS

This work was supported by the National Natural Science Fund of China (Grants 31371476 and 81330041 to Y.T.Z.), the Zhejiang Provincial Natural Science Foundation of China (Grants LY13C070002 to Y.T.Z. and LY13C070001 to Y.L.), Fundamental Research Funds for the Central Universities (Grant 2013QNA7002 to Y.T.Z.), and the Mechanobiology Institute of Singapore (funded through the National Research Foundation and the Ministry of Education Singapore, to B.C.L.).

REFERENCES

Abmayr SM, Pavlath GK (2012). Myoblast fusion: lessons from flies and mice. Development 139, 641–656.

Aoyama T, Hata S, Nakao T, Tanigawa Y, Oka C, Kawaichi M (2009). Cayman ataxia protein caytaxin is transported by kinesin along neurites through binding to kinesin light chains. J Cell Sci 122, 4177–4185.

Bentzinger CF, Wang YX, Rudnicki MA (2012). Building muscle: molecular regulation of myogenesis. Cold Spring Harb Perspect Biol 4, a008342.

Blasius TL, Cai D, Jih GT, Toret CP, Verhey KJ (2007). Two binding partners cooperate to activate the molecular motor Kinesin-1. J Cell Biol 176, 11–17.

Bracale A, Cesca F, Neubrand VE, Newsome TP, Way M, Schiavo G (2007). Kidins220/ARMS is transported by a kinesin-1-based mechanism likely to be involved in neuronal differentiation. Mol Biol Cell 18, 142–152.

Buckingham M (2006). Myogenic progenitor cells and skeletal myogenesis in vertebrates. Curr Opin Genet Dev 16, 525–532.

Buschdorf JP, Li Chew L, Zhang B, Cao Q, Liang FY, Liou YC, Zhou YT, Low BC (2006). Brain-specific BNIP-2-homology protein Caytaxin relocalises glutaminase to neurite terminals and reduces glutamate levels. J Cell Sci 119, 3337–3350.

Cho KI, Cai Y, Yi H, Yeh A, Aslanukov A, Ferreira PA (2007). Association of the kinesin-binding domain of RanBP2 to KIF5B and KIF5C determines mitochondria localization and function. Traffic 8, 1722–1735.

Choudhury A, Dominguez M, Puri V, Sharma DK, Narita K, Wheatley CL, Marks DL, Pagano RE (2002). Rab proteins mediate Golgi transport of caveola-internalized glycosphingolipids and correct lipid trafficking in Niemann-Pick C cells. J Clin Invest 109, 1541–1550.

Cole F, Zhang W, Geyra A, Kang JS, Krauss RS (2004). Positive regulation of myogenic bHLH factors and skeletal muscle development by the cell surface receptor CDO. Dev Cell 7, 843–854.

de Angelis L, Zhao J, Andreucci JJ, Olson EN, Cossu G, McDermott JC (2005). Regulation of vertebrate myotome development by the p38 MAP kinase-MEF2 signaling pathway. Dev Biol 283, 171–179.
Dhanasekaran DN, Kashef K, Lee CM, Xu H, Reddy EP (2007). Scaffold proteins of MAP-kinase modules. Oncogene 26, 3185–3202.
Folker ES, Schulman VK, Baylies MK (2014). Translocating myonuclei have distinct leading and lagging edges that require kinesin and dynein. Development 141, 355–366.
Glater EE, Megeath LJ, Stowers RS, Schwarz TL (2006). Axonal transport of mitochondria requires milton to recruit kinesin heavy chain and is light chain independent. J Cell Biol 173, 545–557.
Good MC, Zalatan JG, Lim WA (2011). Scaffold proteins: hubs for controlling the flow of cellular information. Science 332, 680–686.
Guasconi V, Puri PL (2009). Chromatin: the interface between extrinsic cues and the epigenetic regulation of muscle regeneration. Trends Cell Biol 19, 286–294.
Han J, Jiang Y, Li Z, Kravchenko VV, Ulevitch RJ (1997). Activation of the transcription factor MEF2C by the MAP kinase p38 in inflammation. Nature 386, 296–299.
Harding A, Tian T, Westbury E, Frische E, Hancock JF (2005). Subcellular localization determines MAP kinase signal output. Curr Biol 15, 869–873.
Hirokawa N, Noda Y (2008). Intracellular transport and kinesin superfamily proteins, KIFs: structure, function, and dynamics. Physiol Rev 88, 1089–1118.
Hirokawa N, Noda Y, Tanaka Y, Niwa S (2009). Kinesin superfamily motor proteins and intracellular transport. Nat Rev Mol Cell Biol 10, 682–696.
Hirokawa N, Pfister KK, Yorifuji H, Wagner MC, Brady ST, Bloom GS (1989). Submolecular domains of bovine brain kinesin identified by electron microscopy and monoclonal antibody decoration. Cell 56, 867–878.
Jaulin F, Xue X, Rodriguez-Boulan E, Kreitzer G (2007). Polarization-dependent selective transport to the apical membrane by KIF5B in MDCK cells. Dev Cell 13, 511–522.
Jones NC, Tyner KJ, Nibarger L, Stanley HM, Cornelison DD, Fedorov YV, Olwin BB (2005). The p38alpha/beta MAPK functions as a molecular switch to activate the quiescent satellite cell. J Cell Biol 169, 105–116.
Kanai Y, Okada Y, Tanaka Y, Harada A, Terada S, Hirokawa N (2000). KIF5C, a novel neuronal kinesin enriched in motor neurons. J Neurosci 20, 6374–6384.
Kang JS, Bae GU, Yi MJ, Yang YJ, Oh JE, Takaesu G, Zhou YT, Low BC, Krauss RS (2008). A Cdo-Bnip-2-Cdc42 signaling pathway regulates p38alpha/beta MAPK activity and myogenic differentiation. J Cell Biol 182, 497–507.
Kang JS, Feinleib JL, Knox S, Ketteringham MA, Krauss RS (2003). Promyogenic members of the Ig and cadherin families associate to positively regulate differentiation. Proc Natl Acad Sci USA 100, 3989–3994.
Kang JS, Mulieri PJ, Hu Y, Taliana L, Krauss RS (2002). BOC, an Ig superfamily member, associates with CDO to positively regulate myogenic differentiation. EMBO J 21, 114–124.
Kang JS, Mulieri PJ, Miller C, Sassoon DA, Krauss RS (1998). CDO, a robo-related cell surface protein that mediates myogenic differentiation. J Cell Biol 143, 403–413.
Knight JD, Kothary R (2011). The myogenic kinome: protein kinases critical to mammalian skeletal myogenesis. Skeletal Muscle 1, 29.
Krauss RS, Cole F, Gaio U, Takaesu G, Zhang W, Kang JS (2005). Close encounters: regulation of vertebrate skeletal myogenesis by cell-cell contact. J Cell Sci 118, 2355–2362.
Low BC, Lim YP, Lim J, Wong ES, Guy GR (1999). Tyrosine phosphorylation of the Bcl-2-associated protein BNIP-2 by fibroblast growth factor receptor-1 prevents its binding to Cdc42GAP and Cdc42. J Biol Chem 274, 33123–33130.
Low BC, Seow KT, Guy GR (2000). The BNIP-2 and Cdc42GAP homology domain of BNIP-2 mediates its homophilic association and heterophilic interaction with Cdc42GAP. J Biol Chem 275, 37742–37751.
Marshall CJ (1995). Specificity of receptor tyrosine kinase signaling: transient versus sustained extracellular signal-regulated kinase activation. Cell 80, 179–185.
Metzger T, Gache V, Xu M, Cadot B, Folker ES, Richardson BE, Gomes ER, Baylies MK (2012). MAP and kinesin-dependent nuclear positioning is required for skeletal muscle function. Nature 484, 120–124.
Miaczynska M, Bar-Sagi D (2010). Signaling endosomes: seeing is believing. Curr Opin Cell Biol 22, 535–540.
Osmani N, Peglion F, Chavrier P, Etienne-Manneville S (2010). Cdc42 localization and cell polarity depend on membrane traffic. J Cell Biol 191, 1261–1269.
Palamidessi A, Frittoli E, Garre M, Faretta M, Mione M, Testa I, Diaspro A, Lanzetti L, Scita G, Di Fiore PP (2008). Endocytic trafficking of Rac is required for the spatial restriction of signaling in cell migration. Cell 134, 135–147.
Pan CQ, Low BC (2012). Functional plasticity of the BNIP-2 and Cdc42GAP Homology (BCH) domain in cell signaling and cell dynamics. FEBS Lett 586, 2674–2691.
Pan CQ, Sudol M, Sheetz M, Low BC (2012). Modularity and functional plasticity of scaffold proteins as p(l)acemakers in cell signaling. Cell Signal 24, 2143–2165.
Puri PL, Wu Z, Zhang P, Wood LD, Bhakta KS, Han J, Feramisco JR, Karin M, Wang JY (2000). Induction of terminal differentiation by constitutive activation of p38 MAP kinase in human rhabdomyosarcoma cells. Genes Dev 14, 574–584.
Ravichandran A, Low BC (2013). SmgGDS antagonizes BPGAP1-induced Ras/ERK activation and neuritogenesis in PC12 cell differentiation. Mol Biol Cell 24, 145–156.
Rochlin K, Yu S, Roy S, Baylies MK (2010). Myoblast fusion: when it takes more to make one. Dev Biol 341, 66–83.
Setou M, Seog DH, Tanaka Y, Kanai Y, Takei Y, Kawagishi M, Hirokawa N (2002). Glutamate-receptor-interacting protein GRIP1 directly steers kinesin to dendrites. Nature 417, 83–87.
Siebrands CC, Sanger JM, Sanger JW (2004). Myofibrillogenesis in skeletal muscle cells in the presence of taxol. Cell Motil Cytoskeleton 58, 39–52.
Sirokmany G, Szidonya L, Kaldi K, Gaborik Z, Ligeti E, Geiszt M (2006). Sec14 homology domain targets p50RhoGAP to endosomes and provides a link between Rab and Rho GTPases. J Biol Chem 281, 6096–6105.
Stenmark H (2009). Rab GTPases as coordinators of vesicle traffic. Nature reviews. Mol Cell Biol 10, 513–525.
Sun F, Zhu C, Dixit R, Cavalli V (2011). Sunday Driver/JIP3 binds kinesin heavy chain directly and enhances its motility. EMBO J 30, 3416–3429.
Takaesu G, Kang JS, Bae GU, Yi MJ, Lee CM, Reddy EP, Krauss RS (2006). Activation of p38alpha/beta MAPK in myogenesis via binding of the scaffold protein JLP to the cell surface protein Cdo. J Cell Biol 175, 383–388.
Tapscott SJ (2005). The circuitry of a master switch: Myod and the regulation of skeletal muscle gene transcription. Development 132, 2685–2695.
Vale RD, Reese TS, Sheetz MP (1985). Identification of a novel force-generating protein, kinesin, involved in microtubule-based motility. Cell 42, 39–50.
Verhey KJ, Hammond JW (2009). Traffic control: regulation of kinesin motors. Nat Rev Mol Cell Biol 10, 765–777.
Vonderheit A, Helenius A (2005). Rab7 associates with early endosomes to mediate sorting and transport of Semliki forest virus to late endosomes. PLoS Biol 3, 1225–1238.
Wang Z, Cui J, Wong WM, Li X, Xue W, Lin R, Wang J, Wang P, Tanner JA, Cheah KS, *et al*. (2013). Kif5b controls the localization of myofibril components for their assembly and linkage to the myotendinous junctions. Development 140, 617–626.
Wilson MH, Holzbaur EL (2012). Opposing microtubule motors drive robust nuclear dynamics in developing muscle cells. J Cell Sci 125, 4158–4169.
Wozniak MJ, Allan VJ (2006). Cargo selection by specific kinesin light chain 1 isoforms. EMBO J 25, 5457–5468.
Wu Z, Woodring PJ, Bhakta KS, Tamura K, Wen F, Feramisco JR, Karin M, Wang JY, Puri PL (2000). p38 and extracellular signal-regulated kinases regulate the myogenic program at multiple steps. Mol Cell Biol 20, 3951–3964.
Yang JT, Laymon RA, Goldstein LS (1989). A three-domain structure of kinesin heavy chain revealed by DNA sequence and microtubule binding analyses. Cell 56, 879–889.
Zhou YT, Chew LL, Lin SC, Low BC (2010). The BNIP-2 and Cdc42GAP homology (BCH) domain of p50RhoGAP/Cdc42GAP sequesters RhoA from inactivation by the adjacent GTPase-activating protein domain. Mol Biol Cell 21, 3232–3246.
Zhou YT, Guy GR, Low BC (2005). BNIP-2 induces cell elongation and membrane protrusions by interacting with Cdc42 via a unique Cdc42-binding motif within its BNIP-2 and Cdc42GAP homology domain. Exp Cell Res 303, 263–274.
Zhou YT, Guy GR, Low BC (2006). BNIP-Salpha induces cell rounding and apoptosis by displacing p50RhoGAP and facilitating RhoA activation via its unique motifs in the BNIP-2 and Cdc42GAP homology domain. Oncogene 25, 2393–2408.
Zhou YT, Soh UJ, Shang X, Guy GR, Low BC (2002). The BNIP-2 and Cdc42GAP homology/Sec14p-like domain of BNIP-Salpha is a novel apoptosis-inducing sequence. J Biol Chem 277, 7483–7492.